vol. 63, no. 5, pp. 337–340, 1990.
[19] Y. Takefuji, L. L. Chen, K. C. Lee, and J. Huffman, "Parallel algorithms for finding a near-maximum independent set of a circle graph," *IEEE Trans. Neural Networks*, vol. 1, pp. 263–267, 1990.
[20] Y. Takefuji and K. C. Lee, "An artificial hysteresis binary neuron: A model suppressing the oscillatory behaviors of neural dynamics," *Biol. Cybern.*, vol. 64, pp. 353–356, 1991.
[21] N. Funabiki and Y. Takefuji, "A parallel algorithm for time slot assignment problems in TDM hierarchical switching systems," *IEEE Trans. Commun.*, to be published.
[22] ——, "A parallel algorithm for channel routing problems," *IEEE Trans. Computer-Aided Design*, vol. 11, pp. 464–474, Apr. 1992.
[23] ——, "A parallel algorithm for solving the Hip games," *Neurocomputing*, vol. 3, pp. 97–106, 1991.
[24] Y. Takefuji and K. C. Lee, "Artificial neural networks for four-coloring problems and k-colorability problems," *IEEE Trans. Circuits and Systems*, vol. 38, pp. 326–333, 1991.
[25] N. Funabiki and Y. Takefuji, "A parallel algorithm for spare allocation problems," *IEEE Trans. Reliability*, vol. 40, pp. 338–346, 1992.
[26] Y. Takefuji, *Neural Network Parallel Computing*. Amsterdam, The Netherlands: Kluwer-Academic, Jan. 1992.

Knowledge-Guided Visual Perception of 3-D Human Gait from a Single Image Sequence

Zen Chen and Hsi-Jian Lee

Abstract—**A computer vision method is presented to determine the 3-D spatial locations of joints or feature points of a human body from a film recording the human motion during walking. The proposed method first applies the geometric projection theory to obtain a set of feasible postures from a single image, then it makes use of the given dimensions of the human stick figure, physiological and motion-specific knowledge to constrain the feasible postures in both the single-frame analysis and the multi-frame analysis. Finally a unique gait interpretation is selected by an optimization algorithm. Computer simulations are used to illustrate the ideas presented.**

I. Introduction

In the past a large amount of work has been devoted to problems of human locomotion, notably walking [1]–[3]. In the human gait analysis the entire body motion during walking is represented as a set of spatial trajectories of joints (or anatomic points) [4]–[7]. The mechanics of joint forces and moments is characterized by angular accelerations, velocities and displacements [2], [8]–[9]. Typical application fields of the gait analysis include the physical therapy of joint diseases, biomechanical simulations, kinesiological analysis and mobile robot design, etc. [2], [10]–[11].

There are two major vision methods: stereo vision and monocular vision. In the stereo vision at least two views of the subject are simultaneously taken, then a triangulation method is applied to these views to compute the 3-D coordinates for those joints appearing in two views simultaneously [12]–[13]. On the other hand, the monocular vision can determine the 3-D motion and structure (unique up to a scaling factor) of the subject based on a number of consecutive frames [14]–[17]. Both approaches have their own advantages and shortcomings [18].

In the human gait analysis, the stereo vision can determine the joint positions without using any *a priori* knowledge. Since the triangulation method completely relies on the two vectors defined by the viewpoints and projected points, any digitization error of projected points will lead to an inaccurate joint position. This is true especially when the two vectors are nearly parallel to each other. As a consequence, the obtained joint positions may not represent the legal (i.e., original) human body model. Furthermore, it is difficult to use any knowledge about the human model to refine the result in the stereo vision method. Therefore, for the well-constrained human body model, the stereo vision may not be suitable.

As to the monocular vision, the method requires a sufficient number of joints on the subject to appear in consecutive frames. It is generally impossible to have so many points for human body segments such as arms and legs. Besides, only the structure, unique up to a scaling factor, can be obtained instead of the exact body position. In the field of the robot vision there are methods that can directly determine the 3-D locations of the subject, if the dimensions of the subject is known beforehand [19]–[20]. However, in these methods some viewing conditions or object structure conditions are assumed; it is not very realistic in the human gait analysis. So far there have been only partial solutions to the visual interpretation problem of the general human motion data [17], [21]–[22].

Up to now only geometrical and topological models of a human body are employed in the gait interpretation which generally lead to nonunique joint position recovery from the film. Rashid [21] indicated that the object topology and world knowledge are required to help the interpretation. Herman [23] tried to obtain a meaningful description of a human body motion while playing baseball by using domain-dependent knowledge about the body model. O'Rourke and Badler [22] used constraints of the human body model such as distance constraints, joint angle limits, collision avoidance to refine the 3-D joint positions. In a previous study, we also used physiological and motion specific constraints to derive a small set of feasible body postures for a single frame [7]. Therefore, the application of various sources of knowledge will reduce the joint position ambiguity and can lead to a small set of candidate solutions.

It is not very meaningful to describe a human motion with only a single frame. Instead, the human motion is better described by a collection of consecutive frames as a whole. Hence, certain candidate solutions obtained in the single-frame analysis may be ruled out by checking the interframe compatibility or consistency pertinent to the motion analysis.

In this study a computer vision method for interpreting the human motion during walking is presented. In Section II basic analyses for gait interpretations are described which lead to a set of possible interpretations. Then a computational model based on a graph search theory is formulated for finding a unique interpretation solution in Section III. Algorithm A^* with a proper evaluation function is proposed to find the solutions. Two sets of experimental data are used in the simulation. The algorithm and simulation results are given in Section IV. The results indicate that the algorithm has some minor defects. In Section V two modifications are made to Algorithm A^*. After these changes, together with the aid of additional motion-specific knowledge, a final unique gait interpretation is reached. The simulation results show the goodness of the method. Section VI gives the conclusion.

Manuscript received March 31, 1989; revised September 8, 1989, and May 22, 1991.

The authors are with the Department of Computer Science and Information Engineering, National Chiao Tung University, Hsinchu, Taiwan, 30050 R.O.C.

IEEE Log Number 9104117.

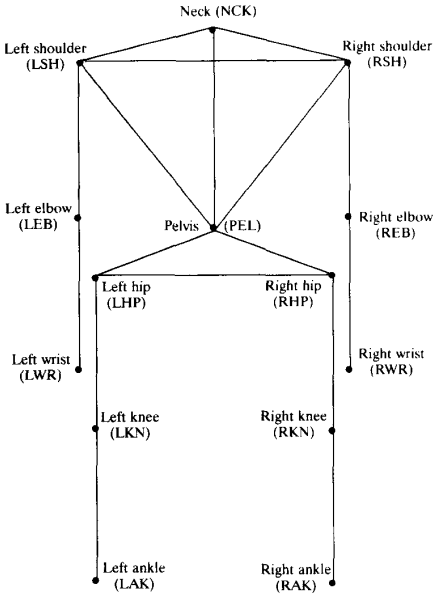

Fig. 1. A stick-figure human body model.

II. Basic Analyses for Gait Interpretations

A. Position Determination of a Jointed Body

A human body is considered as a jointed object, consisting of a number of subparts: head, torso, hip, arms and legs. Each subpart is assumed to be rigid and is characterized by a set of feature points. A body model adopted here as well as in a previous study [7] is shown in Fig. 1. It contains 14 joints and 17 segments; the head above the neck is not shown. There are six or more feature points on the head: neck, nose, two eyes, two ears and chin, etc. Assume that the lengths of all (rigid) segments, plus the relative locations of the feature points on the head, are given beforehand.

1) Single-Frame Analysis: The numbers of available feature points on subparts are different: six (or more) for the head, four for the torso, three for the hip, arms and legs. The possibility of using the geometrical projection theory to recover the subpart location depends on the number of feature points available. It is possible to find the relative location of a rigid part with respect to the camera coordinate system, if the rigid part contains six or more known feature points [24]. After the feature points of the head are determined, the possible locations of feature points on other subparts can be determined from joint to joint in a transitive manner [7]. It is shown that there are generally two possible solutions for the 3-D coordinates values of a feature point under the condition that the segment has a given length. The possible solutions of the feature points can be represented by an interpretation tree, as shown in Fig. 2. There are 2^{n-1} or less possible body configurations or postures where n is the number of joints.

2) Tree Pruning by Using World Knowledge: Not all of the 2^{n-1} body configurations are possible in the real world. Various sources of knowledge can be used to prune the interpretation tree [7]. The physiological knowledge in the form of joint angle constraints, fixed distance constraints, and segment length constraints can be applied to eliminate a great number of infeasible solutions. In addition, the general walking-model constraints such as the following rules can be applied to further reduce the number of possible solutions:

Rule 1: The two arms cannot be both in front of or behind the torso simultaneously. The same restriction also holds for the two legs.

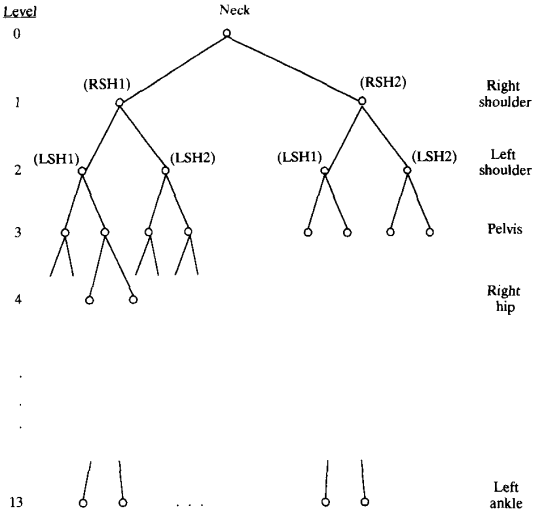

Fig. 2. An interpretation tree for joint position determination.

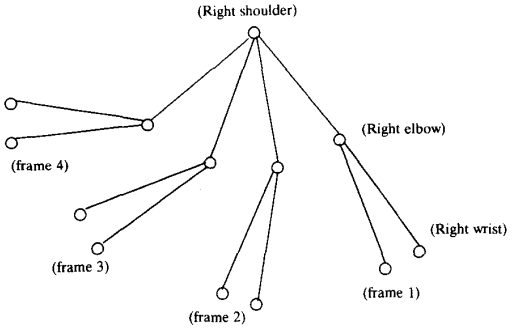

Fig. 3. The possible configurations of the right arm during swinging.

Rule 2: The arm and the leg which are on the same side of the body cannot swing forward or backward at the same time.

B. Motion Analysis Using Multiple Frames

The solutions obtained for all single frames can be combined to determine whether or not they constitute a legal motion. It has been argued [25] that because of the passive viscoelastic and active chemicomechanical properties of muscle, the muscular movement during walking is constrained to proceed in a relatively smooth, continuous fashion. The relatively smooth, continuous motion also means a steady consumption of body energy at the joints (i.e., without any abrupt change in joint torques). It is for this reason that a legal or normal walking means a relatively smooth, continuous motion.

In Fig. 3 we give an example to show how to use the multi-frame analysis to remove some illegal solutions obtained in the single-frame analysis. Assume that the number of possible configurations of the right arm is two for frames 1 and 2, and one for frames 3 and 4. These four consecutive frames constitute a partial cycle of the right arm motion during walking. It can be seen that the relatively smooth angular motion of the lower arm from frame 3 to frame 4 indicates that the correct solutions for the right arm in frames 1 and 2 are those bent arms instead of the stretched ones. Thus, the unique solutions for frames 1 and 2 are obtained through the motion analysis.

Thus the legal motion recorded in consecutive frames corresponds

to the correct transition path of the body configurations chosen from the frames. And a graph search framework can be used to describe the motion analysis that will be presented next.

III. Motion Analysis by Graph Search

A computational model for the motion analysis is needed. With this model, a relatively smooth, continuous trajectory of motion corresponding to the given gait displacement data can be quantitatively defined.

Let variable x_i denote one of the possible body configurations in frame i. Also let $\vec{A}(x_i)$ denote the position vector of joint A $\vec{AB}(x_i)$ denote the vector from joint A to joint B on a segment $\bar{AB}$, all in body configuration x_i. Assume the time interval between two consecutive frames is Δt. Then the relative translational velocity of the segment $\bar{AB}$ from body configuration x_i in frame i to another body configuration x_{i+1} in frame $i+1$ is defined as:

$$\vec{V}_{\bar{AB}}x_i, x_{i+1}) = \{[\vec{B}(x_{i+1}) - \vec{B}(x_i))] - [\vec{A}(x_{i+1}) - \vec{A}(x_i)]\}/\Delta t$$
$$= [\vec{AB}(x_{i+1}) - \vec{AB}(x_i)]/\Delta t.$$

The relative angular velocity and acceleration of segment $\bar{AB}$ are also defined as

$$\vec{\omega}_{\overline{AB}}(x_i, x_{i+1}) = \vec{AB} \times \vec{V}_{\overline{AB}}(x_i, x_{i+1}) \text{ (a cross product)}$$

and

$$\alpha_{\overline{AB}}(x_i, x_{i+1}, x_{i+2}) = |\vec{\omega}_{\overline{AB}}(x_{i+1}, x_{i+2}) - \vec{\omega}_{\overline{AB}}(x_i, x_{i+1})|/\Delta t.$$

The body movement is a process involving rather complicated human dynamics where the internal and external forces act on the skeleton [2]. Nevertheless, the walking motion consists of periodic gait cycles that can be viewed as the individual periodic motions of all body segments linked at joints. In fact, these body segments undergo rotational motions. The rotations of the legs with respect to the ground results in the body translation. To define each individual periodic angular motion of a body segment, the translational component of the body segment is decomposed and subtracted.

A smooth, continuous body movement during walking is now considered as a collection of smooth, continuous angular motions of all body segments. In addition, a smooth angular motion of a body segment during walking indicates a nearly constant angular velocity, or equivalently, a nearly zero angular acceleration. Thus, to measure the smoothness of a walking motion during frames $i, i+1$, and $i+2$, we define an angular acceleration function associated with body configurations x_i, x_{i+1}, x_{i+2} as:

$$f_i(x_i, x_{i+1}, x_{i+2}) = \sum_{\overline{AB}} |\vec{\alpha}_{\overline{AB}}(x_i, x_{i+1}, x_{i+2})|,$$

where the summation is taken over all body segments and the magnitudes of angular accelerations are used for simplicity. Next, the overall angular acceleration function defined over N frames is given as

$$f(x_1, x_2, \cdots x_N) = f_1(x_1, x_2, x_3) + f_2 x_2, x_3, x_4)$$
$$+ \cdots + f_{N-2}(x_{N-2}, x_{N-1}, x_N).$$

Theoretically speaking, to find a smooth spatial trajectory from the given N frames of human motion data during walking is equivalent to finding a solution to $f(x_1, x_2, \cdots, x_N)$ with the smallest value (or, to be more realistic, with a nearly smallest value).

The problem of finding the smallest value of $f(x_1, x_2, \cdots, x_N)$ can be formulated as a graph search problem. Here a multistage biframe transition graph similar to the graph used by Martelli [26] is defined below.

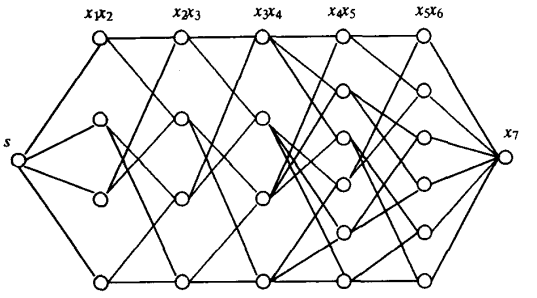

Fig. 4. A multistage biframe transition graph.

In Fig. 4 a multistage biframe graph for recovered body configurations corresponding to a gait cycle of six consecutive frames is illustrated. A start node s is added at stage zero. It is the head of the biframe transition graph. The nodes at stage 1 correspond to the body configurations of frames 1 and 2, represented by the pair of variables x_1 and x_2. The nodes at stage 2 correspond to the combinations of body configurations of frames 2 and 3, represented by the pair of variables x_2 and x_3. Since x_2 and x_3 interact with x_1 through function $f_1(x_1, x_2, x_3)$, there will be an edge between the nodes at stage 1 and stage 2, if the values of variable x_2 of the two stages are the same. The nodes and edges at subsequent stages are constructed in the same manner.

IV. Finding Gait Solutions By Algorithm A*

A. Algorithm A* with an Evaluation Function

Algorithm A* can be effective in finding the optimal solution to the graph search problem, if a suitable evaluation function is defined. The evaluation function consists of two functions g and h. The $g(n)$ function associated with a node n is defined to be the estimated cost from the start node s to the node n. In our application, the g value of a biframe node (x_i, x_{i+1}) is given by

$$g_1(x_1, x_2) = 0$$

and

$$g_i(x_i, x_{i+1}) = g_{i-1}(x_{i-1}, x_i) + f_{i-1}(x_{i-1}, x_i, x_{i+1}) \text{ for } i \geq 2.$$

After the recursive substitution, the function g can be expressed as

$$g_i(x_i, x_{i+1}) = f_1(x_1, x_2, x_3) + f_2(x_2, x_3, x_4)$$
$$+ \cdots + f_{i-1}(x_{i-1}, x_i, x_{i+1}).$$

It is the sum of acceleration functions along the transition path from the start node to node (x_i, x_{i+1}).

On the other hand, the value of the heuristic function $h(n)$ is defined to be the estimated cost from node n to a goal node. In this study, the $h(x_i, x_{i+1})$ value at node (x_i, x_{i+1}) is defined as

$$h(x_i, x_{i+1}) = \min_{x_{i+2}}[f_i(x_i, x_{i+1}, x_{i+2})]$$
$$+ \min_{x_{i+2}, x_{i+3}}[f_{i+1}(x_{i+1}, x_{i+2}, x_{i+3})]$$
$$+ \sum_{k=i+2}^{N-2} [\min_{x_k, x_{k+1}, x_{k+2}} f_k(x_k, x_{k+1}, x_{k+2})].$$

For the h function defined previously, it can be easily shown that the h function satisfies the *admissible constraint*, that is, $h(x_i, x_{i+1}) \leq h^*(x_i, x_{i+1})$, where h^* is the optimal h value. Also,

TABLE I
OPTIMAL TRANSITION PATHS FOUND BY ALGORITHM A*
A—FOR THE FIRST IMAGE SEQUENCE POS1

Parameter No.	Starting-frame, Ending-frame, Max Number of Transitions	Number of Nodes Expanded	Total Cost	Optimal Transition Path Specified by Body Conf. in Each Frame
1	(1,9,5)	209	1871.64	(6,6,2,2,2,1,1,9,1)
2	(1,9,3)	84	1871.64	(6,6,2,2,2,1,1,9,1)

B—FOR THE SECOND IMAGE SEQUENCE POS2

Parameter No.	Starting-frame, Ending-frame, Max Number of Transitions	Number of Nodes Expanded	Total Cost	Optimal Transition Path Specified by Body Conf. in Each Frame
1	(1,18,5)	121	3307.1	(4,13,4,4,3,15,5,2,3,3,3,3,6,6,13,6,6,5)
2	(1,18,8)	70	3118.2	(4,13,4,4,3,23,7,2,3,3,3,3,6,6,7,6,6,5)

the h function satisfies the condition of monotone restriction[27]. That is, for every node (x_{i+1}, x_{i+2}) that is a successor of node (x_i, x_{i+1}),

$$h(x_i, x_{i+1}) - h(x_{i+1}, x_{i+2}) \leq f_i(x_i, x_{i+1}, x_{i+2}).$$

With this property, we have $g(n) = g^*(n)$, the optimal g value at node n, for any expanded node n. Namely, the node expansion process will not have any parentage redirection, so it will be more efficient.

In the application of algorithm A*, the available number of node expansions due to the possible transitions between two consecutive frames may be quite large. To reduce the memory size and computational time required, it is a common practice to restrict the maximum number of transitions between two consecutive frames to a fixed number, say, k. Here the first k smallest sums of relative angular displacements between all possible pairings of body configurations of two consecutive frames are found. These k transitions are then used in the node expansion process of algorithm A*.

B. Simulation Results and Discussions

Two experiments are conducted to test the goodness of algorithm A*. Each experiment uses a single input image sequence. The first experiment uses an image sequence, IMG1, that is the perspective views of 3D human walking data (generated initially by Cutting[28]), taken by a camera located in front of the walking man. And the second experiment used another input image sequence, IMG2, that is taken with the camera located in front, but to the right of the walking man. In each experiment, the single-frame analysis [7] is performed first to obtain the set of recovered body configurations from each frame of the input image data. Denote the collection of recovered body configurations in the sequence of all frames as POS1 for the first experiment and POS2 for the second experiment.

In each experiment two different sets of control parameters are used that specify the starting and ending frames of the input image data used and the maximum number of allowable transitions, k, considered in the graph search process. Table I gives the optimal transition paths found by algorithm A* for the two experiments with the given different sets of control parameters. From this table the obtained optimal transition paths with the two different control parameters are the same for the sequence POS1 and quite similar for the sequence POS2.

Now we compare the results with the actual input image data. Fig. 5 shows the projected view of the body configurations of the given input image sequence IMG1 and that of the optimal transition path found by Algorithm A* from the given input data, all in the camera-centered $z_c y_c$ coordinate system with the z_c axis being the optical axis. It can be seen that these two sets of body configurations are remarkably in agreement. Table II gives the mean and variance values of the joint position errors between the recovered positions and actual positions in the 3D space over all frames. These values are rather small for all joints except the joints of the right lower arm and of the left lower leg in frame 7. This partial disagreement will be overcome in a later section by the application of motion-specific knowledge.

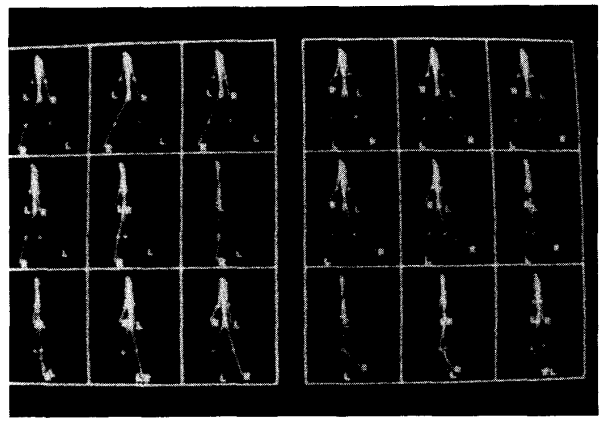

Fig. 5. The projected views of the body configurations in the $z_c y_c$ camera-centered coordinate system corresponding to (a) the input image sequence IMG1, and (b) the optimal transition path found by algorithm A* for the data set POS1(1, 9, 5).

One the other hand, the recovered body configurations in the second experiment POS2(1,18,5) are almost correct except that both arms swing in a direction not parallel to the walking direction. Figs. 6 and 7 show the projected view of the body configurations of the given input image sequence IMG2 and that of the optimal transition path found by algorithm A*. It can be seen that in Fig. 7 either arm swings in a direction different from that shown in Fig. 6. Table III shows that the mean and variance values of the two wrist joint positions are relatively large.

The possible reasons for the previous disagreements at a few joints in the two experiments include the following.

1) The true solution, as will be seen later, may have a total cost slightly larger than that of the optimal transition path, so the optimal solution is theoretically the best one, but it may only be close to the true solution.
2) The allowable transitions in the graph search process are

TABLE II
THE MEAN AND VARIANCE VALUES OF ALL JOINT POSITION ERRORS FOR THE TRANSITION PATH FOUND BY ALGORITHM A* FOR THE DATA SET POS1 (1, 9, 5)

	Mean	Variance
Neck	0.09	0.00
Right shoulder	1.20	0.80
Left shoulder	1.49	0.81
Right elbow	2.38	9.73
Left elbow	2.07	2.15
Right wrist	3.03	13.86
Left wrist	2.57	3.12
Pelvis	0.76	0.28
Right hip	1.68	2.46
Left hip	1.48	1.38
Right knee	1.32	1.75
Left knee	1.95	5.65
Right ankle	1.16	2.13
Left ankle	1.86	5.01

TABLE III
THE MEAN AND VARIANCE VALUES OF ALL JOINT POSITION ERRORS FOR THE TRANSITION PATH FOUND BY ALGORITHM A* FOR THE DATA SET POS2 (1, 18, 5)

	Mean	Variance
Neck	0.53	0.28
Right shoulder	0.48	0.28
Left shoulder	0.39	0.16
Right elbow	1.07	3.33
Left elbow	0.55	0.40
Right wrist	12.62	47.92
Left wrist	9.69	44.55
Pelvis	1.33	1.33
Right hip	1.62	1.62
Left hip	1.25	1.25
Right knee	1.84	4.29
Left knee	0.95	0.95
Right ankle	2.39	11.51
Left ankle	1.38	1.49

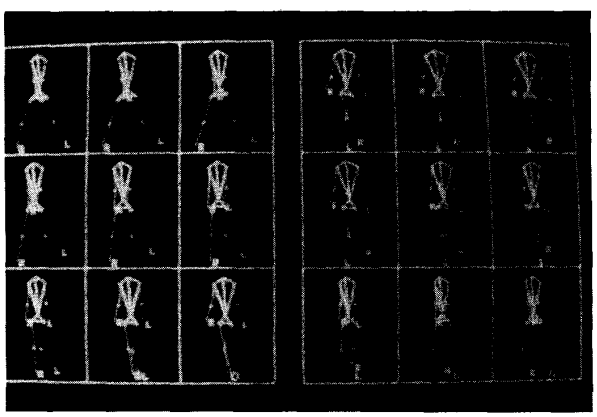

Fig. 6. The projected views of the body configurations of the input image sequence IMG2.

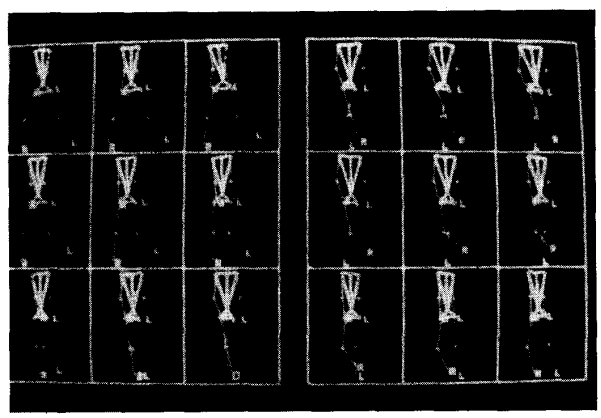

Fig. 7. The projected views of the optimal transition path found by algorithm A* for the data set POS2(1, 18, 5).

restricted to those with the first k smallest sums of relative angular displacements. It will be seen later that the correct transitions between frames may not always be among the assumed first k transitions.

In the next section we shall modify algorithm A* so that the previous two drawbacks can be overcome in order to generate the true solution.

V. SOLUTION REFINEMENT WITH KNOWLEDGE

A. Modifications of Algorithm A*

In order to obtain more than one solution path, one modification of algorithm A* is to abandon the restriction of a single parentage of a node, since multiple solution paths may meet at a node. To do so, during the node expansion process the entire path obtained up to a node will be recorded at the node instead of just its most recent parentage. Therefore, if there are two or more paths leading to a node, there will be the same number of path lists recorded at the node. The other aspects of algorithm A* remain the same, although some possible simplifications can be made, if desired. The total number of solution paths to be found is based on the maximum deviation from an optimal value that an acceptable solution path can have.

We also make another modification about the frame transitions used in the algorithm. Recall that there are generally two possible solutions for each joint of a body configuration. These two solutions are labeled as F (for the one close to the camera) and R (for the one farther away from the camera). In case that there is only one degenerate solution, it will be labeled as D (for the degenerate solution). The joint transition will be determined based on the distance between the F and R candidate solutions, called the FR distance. The new possible joint transitions in the graph are given as follows.

1) When the FR distance of a joint is larger than a prespecified threshold, then the F/R label of the joint must remain the same as that in the previous frame.
2) When the FR distance of a joint is less than the prespecified threshold, then the F/R label of the joint of the next frame can be of either type. These conditions for joint transitions between two consecutive frames eliminate those transitions with a large change in the joint angular displacement. This is appropriate under the assumption of smooth walking.

B. Solution Improvement by the Revised Algorithm A*

We apply the revised algorithm A* to the same two input data sets. The results show great improvements.

Table IV shows the first and the eighth optimal transition paths found by the application of the revised algorithm A* to the image data POS1 with a control parameter set (1, 9, *new*) where *new* indicates the new rules for frame transition mentioned previously. Table V is

TABLE IV
THE FIRST AND THE EIGHTH OPTIMAL TRANSITIONS PATHS FOUND BY THE REVISED ALGORITHM A* FOR THE DATA SET POS1(1,9, *new*)

(1,9,*new*)	Total Cost	Transition Path Specified by Body Configurations
Path #1	1406.49	(22,22,12,22,21,2,77,12,4)
Path #8	1462.59	(6,6,2,2,2,1,76,9,1)

TABLE V
THEMEAN AND VARIANCE VALUES OF ALL JOINT DISTANCES FOR THE TRANSITION PATHS FOUND BY THE REVISED ALGORITHM A* FOR THE DATA SET POS1(1, 9, *new*)

Path No.	Path #1		Path #2	
Joint	mean	variance	mean	variance
NCK	0.09	0.00	0.09	0.00
RSH	1.20	0.80	1.20	0.80
LSH	1.49	0.81	1.49	0.81
REB	1.65	2.50	1.65	2.50
LEB	2.07	2.15	2.07	2.15
RWR	2.15	3.92	2.15	3.92
LWR	2.57	3.12	2.57	3.12
PEL	0.76	0.28	0.76	0.28
RHP	3.18	12.24	1.68	2.46
LHP	3.91	18.26	1.48	1.38
RKN	2.25	7.32	1.32	1.75
LKN	3.24	12.97	1.13	0.80
RAK	2.00	5.53	1.16	2.13
LAK	3.11	11.86	1.09	0.73

TABLE VI
THE FIRST THREE OPTIMAL TRANSITION PATHS FOUND BY THE REVISED ALGORITHM A* FOR THE DATA SET POS2(1, 18, *new*)

(1,18,*new*)	Total Cost	Transition Path Specified by Body Configurations
Path #1	2960.76	(3,9,3,3,4,37,8,3,5,5,5,5,10,10,21,8,8,1)
Path #2	2971.84	(3,9,3,3,4,37,8,3,5,5,5,5,10,10,23,9,9,3)
Path #3	2973.04	(5,17,5,5,4,33,7,1,1,1,1,1,2,2,17,6,6,5)

TABLE VII
THE MEAN AND VARIANCE VALUES OF ALL JOINT POSITION ERRORS FOR THE TRANSITION PATHS FOUND BY THE REVISED ALGORITHM A* FOR THE DATA SET OF POS2(1, 18, *new*)

Path No.	Path #1		Path #2		Path #3	
Joint	mean	variance	variance	variance	mean	variance
NCK	0.53	0.28	0.53	0.28	0.53	0.28
RSH	0.48	0.28	0.48	0.28	0.48	0.28
LSH	0.39	0.16	0.39	0.16	0.39	0.16
REB	0.488	0.14	0.48	0.14	0.48	0.14
LEB	0.47	0.31	0.47	0.31	0.47	0.31
RWR	0.60	0.38	0.60	0.38	11.21	46.33
LWR	2.20	12.79	0.61	0.55	2.20	12.79
PEL	0.82	1.33	0.82	1.33	0.82	1.33
RHP	1.43	1.62	1.43	1.62	1.43	1.62
LHP	1.37	1.25	1.37	1.25	1.37	1.25
RKN	1.84	4.29	1.84	4.29	1.84	4.29
LKN	1.43	0.95	1.43	0.95	1.43	0.95
RAK	2.39	11.51	2.39	11.51	2.39	11.51
LAK	1.38	1.49	1.38	1.49	1.38	1.49

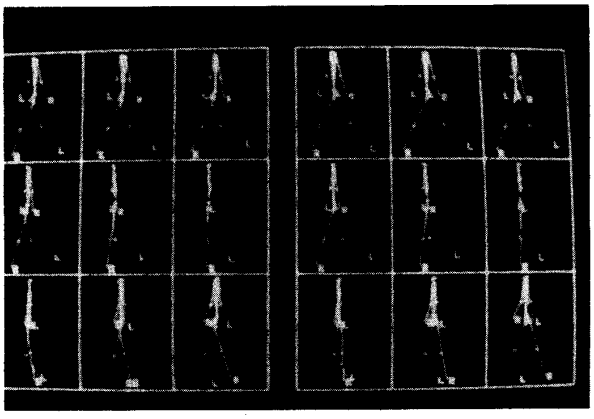

(a) (b)

Fig. 8. The projected views of the solution transition paths found by the revised algorithm A* for the data set POS1(1, 9, *new*). (a) The first transition path, and (b) the eighth transition.

the list of the mean and variance values of all joint position errors for the transition paths found. In comparison with Table I, the new results obtained have the reduced total costs and the eighth optimal transition path has the smallest set of joint position errors. Later on, we shall show that this eighth path fulfills additional desirable motion properties.

We also apply the revised algorithm A* to the second image sequence, POS2. Tables VI and VII give the first three optimal transition paths found and the mean and variance values of all joint position errors. The total costs are also reduced, when compared with the previous experiment. The second optimal transition path has the smallest set of joint position errors.

C. Further Refinement by Additional Motion-Specific Knowledge

The multiple transition paths found by the revised algorithm A* look quite similar to each other, and some are shown in Figs. 8 and 9. To further refine these results we can apply more stringent motion-specific knowledge. Rules 3 through 5 of the walking-model constraint proposed in our previous study [7] are restated here:

Rule 3: When both the shoulder joint and the elbow joint of either arm swing, they must swing in the forward or backward direction simultaneously. The same holds for the hip joint and the knee joint of either leg.

Rule 4: The motion trajectory of either arm or leg is roughly on a plane which is generally parallel to the torso moving direction.

Rule 5: At any time during walking, there is at most one knee having a flexion angle. Moreover, when there is a significant flexion at one leg, then the other leg stands nearly vertically on the ground.

The eighth transition path shown in Fig. 8(b) is checked against Rules 3 to 5 without failure. For the first transition path shown in Fig. 8(a), it can be seen that the left hip violates Rule 3 in the first half of the sequence and that the right hip violates Rule 3 in the second half of the sequence. These observations are confirmed by the statistics of the mean and variance values of joint position errors.

The second transition path shown in Fig. 9 corresponds to the correct motion in which the two arms swing in planes parallel to the walking direction. In the first and the third transition paths, we find that the left arm in the last four frames swings in a direction not parallel to the walking direction. In addition, in the third transition path, the right arm also violates Rule 4.

Therefore, the application of additional motion specific knowledge provides more information to constrain the solution obtained from the multiple-frame analysis. In this way a final gait interpretation is possible to reach.

VI. CONCLUSION

We have presented a computer vision method for interpreting gait displacement data. First, we apply the geometrical projection theory

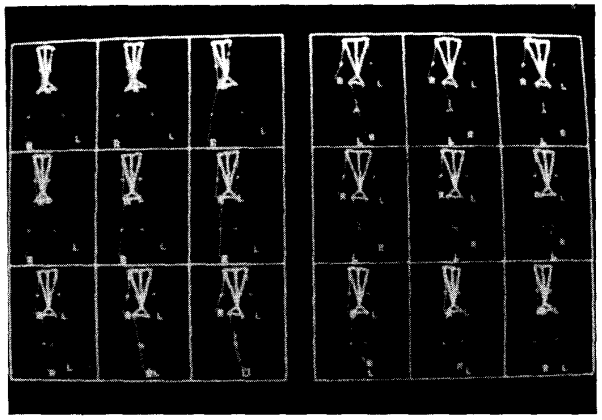

Fig. 9. The projected views of the second transition path found by the revised algorithm A* for the data set POS2(1, 18, *new*).

to find possible postures in each single frame. The physiological knowledge can be used in the filtering process to eliminate infeasible candidates. The correct posture is one among remaining candidates. Then a motion analysis using multiple frames is called. The correct motion corresponds to a right transition path between the candidate postures in the frames, one from each frame. We use a graph search method, algorithm A*, to find the spatial trajectory. We modify algorithm A* to allow multiple optimal solution paths and define new possible frame transitions that satisfy certain conditions imposed by motion smoothness.

The final set of solution paths obtained by the revised algorithm A* is interpreted with more stringent motion specific knowledge that serves to further constrain the solution domain. In this framework an ultimate gait interpretation is obtained. The experiments indicate the effectiveness of using this approach. However, world knowledge including both physiological and motion-specific knowledge may need a more thorough analysis in order to make the best use of it. We are currently considering to use this method to monitor or to aid the control of a multijoint mobile robot. We also consider to apply the same principle with different knowledge to other types of human motion.

REFERENCES

[1] J. B. Morrison, "The mechanics of the knee joint in relation to normal walking," *J. Biomechanics*, vol. 3, pp. 51–61, 1970.

[2] H. Hermami, "A feedback on-off model of biped dynamics," *IEEE Trans. Syst., Man, Cybern.*, vol. SMC-10, pp. 376–383,1980.

[3] H. Hemami and R. L. Farnsworth, "Postural and gait stability of a planar five link biped by simulation," *IEEE Trans. Autom. Contr.*, vol. AC-22, no. 3, pp. 452–458, 1977.

[4] G. Johansson, "Visual perception of biological motion and a model for its analysis," *Perception and Psychophy.*, vol. 14, pp. 201–211,1973.

[5] N. I. Badler and S. W. Smoliar, "Digital representations of human movement," *Computing Surveys*, vol. 11, pp. 19–38, 1979.

[6] D. A. Writer, H. G. Sidwall and D. A. Hobson, "Measurement and reduction of noise in kinematics of locomotion," *J. Biomechanics*, vol. 7, pp. 157–159, 1974.

[7] H. J. Lee and Z. Chen, "Determination of 3D human body postures from a single view," *Computer Vision, Graphics and Image Processing*, vol. 30, pp. 148–168, 1985.

[8] J. C. Pezzack, R. W. Norman and D. A. Winter, "An assessment of derivative determining techniques used for motion analysis," *J. Biomechanics*, vol. 10, pp. 377–382, 1977.

[9] M. S. Ju and J. M. Mansour, "Simulation of the double limb support of human gait," *J. Biomechanical Engr.*, vol. 110, pp. 223–229, 1988.

[10] T. Bajd, *et al.* "The use of a four-channel electrical stimulator as an ambulatory and for paraplegic patients," *Physical Therapy*, vol. 63, no. 7, pp. 1116–1120, 1983.

[11] S. R. Simon, R. M. Nuzzo and M. D. Koskinen, "A comprehensive clinical system for four dimensional motion analysis," *Bull. Hosp. Joint Diseases*, vol. XXXVII, Apr. 1977.

[12] D. B. Genney, "Object detection and measurement using stereo vision", *Proc. 6th Int. Joint Conf. Artif. Intell.*, pp. 320–327, 1979.

[13] S. T. Barnard and M. A. Fischler, "Computational stereo," *Computing Surveys*, vol. 14, pp. 553–572, 1982.

[14] J. W. Roach and J. K. Aggarwal, "Determining the movement of objects from a sequence of images", *IEEE Trans. Pattern. Anal. Mach. Intell.*, vol. PAMI-2, pp. 554–562, 1980.

[15] A. Z. Meiri, "On monocular perception of 3-D moving objects," *IEEE Trans. Pattern. Anal. Mach. Intell.*, vol. PAMI-2, pp. 582–583, 1980.

[16] B. L. Yen and T. S. Huang, "Determining 3-D motion and structure of a rigid body using the spherical projection," *Comp. Vision, Graphics, and Image Processing*, vol. 21, pp. 21–32, 1983.

[17] J. A. Webb and J. K. Aggarwal, "Structure from motion of rigid and jointed objects," *Artificial Intell.*, vol. 19, pp. 107–130, 1982.

[18] S. D. Blostein and T. S. Huang, "Error analysis in stereo determination of 3-D point positions," *IEEE Trans. Pattern Anal. Mach. Intell.*,, vol. PAMI-9, pp. 752–765, 1987.

[19] I. Fukui, "TV image processing to determine the position of a robot vehicle," *Pattern Recog.*, vol. 14, pp. 101–109, 1981.

[20] Z. Chen, D. C. Tseng and J. Y. Lin, "A simple vision algorithm for 3-D position determination using a single calibration object," *Pattern Recognition*, vol. 22, no. 2, pp. 173–187, 1989.

[21] R. F. Rashid, "Toward a system for the interpretation of moving light displays," *IEEE Trans. Pattern Anal. Mach. Intell.*, vol. PAMI-2, pp. 574–581, 1980.

[22] J. O'Rourke and N. I. Badler, "Model-based image analysis of human motion using constraints propagation," *IEEE Trans. Pattern Anal. Mach. Intell.*, vol. PAMI-2, pp. 522–546, 1980.

[23] M. Herman, "Understanding body postures of human stick figures," Ph. D. Dissertation, Univ. Maryland, 1979.

[24] D. F. Rogers and J. A. Adams, *Mathematical Elements for Computer Graphics*. New York: McGraw-Hill, 1978.

[25] R. Jain and I. K. Sethi, "Establishing correspondence of nonrigid objects using smoothness of motions," *Proc. Workshop on Computer Vision: Repres. Contr.*, 1984, pp. 83–87.

[26] A. Martelli, "An application of heuristic search methods to edge contour detection," *Comm. ACM.* vol. 19, pp. 73–83, 1976.

[27] N. J. Nilsson, *Principles of Artificial Intelligence*. Palo Alto, CA: Tioga, 1980.

[28] J. E. Cutting, "A program to generate synthetic walker as dynamic point-light displays," *Behav. RE's. Methods Instrum.*, vol. 10, no. 1, pp. 91–94, 1978.